Nonlinear transport processes and fluid dynamics: Effects of thermoviscous coupling and nonlinear transport coefficients on plane Couette flow of Lennard-Jones fluids

D. K. Bhattacharya and Byung Chan Eu*
Department of Chemistry, McGill University, 801 Sherbrooke Street West, Montreal, Quebec, Canada H3A 2K6
(Received 14 April 1986)

To examine the effects of nonlinear transport processes on the flow properties of a real fluid, we study the plane Couette flow under a temperature gradient in a Lennard-Jones fluid over a range of gas pressure. The analysis is based on the nonlinear transport coefficients derived in the modified moment method. The linear transport coefficients appearing in the theory are those constructed by Ashurst and Hoover from the nonequilibrium molecular-dynamics simulations, while for the equation of state for the Lennard-Jones fluid we use the empirical form proposed by Ree. Examples for the flow characteristics at two extreme conditions when either the gas is very dilute, or when it is very dense, are presented. It is shown that the temperature and velocity profiles for nonlinear transport processes are significantly different from the ones obtained with the linear transport coefficients. In the dilute-gas limit, slip boundary conditions are used which are derived by applying the Langmuir theory of gas-surface interaction. Flow profiles show pronounced boundary-layer structures near the wall when the product of the Knudsen number and the Mach number is sufficiently large.

I. INTRODUCTION

For a macroscopic description of various irreversible transport processes it is essential to know how the dissipative fluxes of mass, momentum, and energy are related to the thermodynamic forces, e.g., gradients of chemical potentials, velocity, and temperature, etc. When the system is close to equilibrium or equivalently when thermodynamic forces are relatively small in magnitude, then the dissipative fluxes are proportional to the thermodynamic forces. Such linear relations of fluxes and thermodynamic forces form the basis of linear irreversible thermodynamics,[1] and the transport processes are said to be linear. If the fluid is isotropic then the thermodynamic forces of different tensorial orders do not couple with each other in the linear domain (the Curie principle). As a consequence, for example, the velocity gradient giving rise to momentum flow does not influence the transport of heat caused by the temperature gradient and vice versa. However, this is no longer true when the system is driven far from equilibrium since then the usual linear flux—thermodynamic-force relations are no longer valid and must be replaced by nonlinear relations. Irreversible thermodynamics for such nonlinear transport processes is termed nonlinear irreversible thermodynamics. In the domain of nonlinear irreversible processes there are intricate couplings of various kinds between different thermodynamic forces, and the evolution of dissipative fluxes is consequently influenced by such couplings. Elucidation of such couplings and the formal structure of nonlinear irreversible thermodynamics is an important subject in nonequilibrium thermodynamics and kinetic theory. A number of irreversible thermodynamics[2] and kinetic-theory investigations have been carried out on the couplings and related questions. In particular, a set of nonlinear transport coefficients has been derived which appears to correlate well with experimental data in various cases so far studied.[3] The fact that there are good correlations between the theoretical nonlinear transport coefficients and experimental data, e.g., rheological data,[3(a),3(b)] carrier mobilities in semiconductors,[3(c)] etc., raises a question as to their implication for the hydrodynamic-flow behavior of the fluid concerned. The question was explored by means of the Maxwell model of gas in a recent paper[4] by one of us (B.C.E.) and his collaborators. It was found that there are significant thermoviscous and nonlinear effects hitherto unobserved. Since the Maxwell model is artificial and confined to low-density gases, it is desirable to remove the limitations of the model, and we have just done that in this paper. The aim of the present investigation is to construct nonlinear transport coefficients by gleaning from the results of kinetic theory[5] and molecular dynamics[6–9] studies on dense fluids and to examine their effects and the influence of nonlinear thermodynamic couplings on the dynamics of plane Couette flow of a viscous heat-conducting dense fluid between two plates at different temperatures. The low-density behavior of the fluid flow is also considered by taking the low-density limits of the transport coefficients and the equation[8,9] of state used. It is found that nonlinear thermodynamic couplings have a significant influence on the velocity and temperature profiles and on the development of boundary layers along the plates, both in the low- and high-density regimes of the fluid.

Before initiating a discussion on the nonlinear evolution equations which form the basis of our analysis it would be useful to comment on some important differences between the kinetic theory underlying the nonlinear evolution

equations used here (the modified moment method) and the classical kinetic theory of transport processes that is based on the Chapman-Enskog method[10] or the moment method[11] for the solution of the Boltzmann equation. Since the Chapman-Enskog and the moment method give basically the same results for the transport coefficients at least in the lower-order approximations we will take the Chapman-Enskog method for this discussion. The Chapman-Enskog method involves the expansion of the distribution function in a power series of the Knudsen number and the coefficients in the series are determined by a perturbation method. If only the first-order terms are retained for the solution there follow linear constitutive (flux-thermodynamic force) relations, and when the latter are substituted into the conservation equations there arise hydrodynamic (Navier-Stokes, Fourier, diffusion) equations. The linear transport coefficients are identified with the coefficients in the linear flux—thermodynamic-force relations, and they, when calculated with a suitable model for interaction potential, are capable of predicting the temperature dependence of transport coefficients in agreement with experiment on sufficiently dilute gases near equilibrium. When second-order terms are taken into consideration we obtain nonlinear constitutive equations (Burnett equation) which are, however, not very useful because of the fact that the solution at this stage is generally not consistent with the second law of thermodynamics insomuch as the entropy production calculated therewith is not necessarily positive definite and thus violates the second law of thermodynamics. This therefore raises a doubt as to the possible utility of the higher-order Chapman-Enskog approximation for providing a transport theory of nonlinear irreversible processes that is consistent with thermodynamics laws. Still another fundamental limitation of the Chapman-Enskog method lies in the fact that the perturbation solution in powers of the Knudsen number ($\underline{K}$) may not converge as the Knudsen number is increased. (The series in fact may be regarded as an asymptotic series.) Such a large Knudsen number arises when the gas is so dilute that the mean free path of molecules is larger than the characteristic dimension of the dissipative system. The mean free path may be regarded as the effective distance over which the momentum and the energy are transported through collisions of particles in an imaginary layer of the fluid with those in another. In this interpretation the "mean free path" may also be large in the case of dense fluids where in spite of the fact that particles are relatively closely packed (thus the free paths of binary collisions may be of the order of molecular size) the frequency of collisions is much increased so that the effective length of momentum or energy transfer per unit time is accordingly increased, thus giving rise to a large viscosity or heat conductivity. As a consequence of the large Knudsen number, the description of the nonlinear fluid behavior exhibited by a very dilute or dense gas in such a condition remains beyond the capability of the Chapman-Enskog method.

If the Boltzmann equation is suitably scaled with characteristic times such as the mean free time and the relaxation time and also with the mean free path and the characteristic length of the system, one finds that the collision integral (term) in the Boltzmann equation is scaled by an inverse Knudsen number. Since $\underline{K}$ tends to infinity as the density vanishes the collision term is often dropped from the Boltzmann equation for studying the dynamics[12] of a gas in the rarefied regime of density and the resulting kinetic equation is solved with suitable boundary conditions imposed on the distribution function. The collisionless Boltzmann equation, however, is nondissipative since the entropy production is identically equal to zero, and yet as we are well aware of, even a rarefied gas is dissipative since there are dissipative processes known to occur. Since there is no intrinsic dissipative mechanism built into the kinetic equation owing to the neglected collision term, the dissipation observed must be attributed solely to the boundary effects, but they cannot be the entirety of the cause for the dissipation in the system. We believe that the limit of large $\underline{K}$ must be taken after the Boltzmann equation is appropriately solved, but not before. In the Bhatnagar-Gross-Krook (BGK) approach[10(b),12] to rarefied-gas dynamics a linearized Boltzmann equation is employed, which certainly removes the defect of nondissipative feature manifest in the collisionless Boltzmann equation. However, the linearization of the collision term is mathematically motivated to make the analysis more tractable. It is preferable to avoid the linearization of the collision term in the Boltzmann equation. This demands a more careful treatment of the kinetic equation and the modified moment method is designed for that kind of purpose among others.

The above-mentioned limitations of conventional kinetic theory could be overcome by solving the Boltzmann equation with the modified moment method.[2] In this method the kinetic equation such as the Boltzmann equation or its dense-fluid generalization[5] is solved in a way fully consistent with the thermodynamic laws at every order of approximation taken for calculating transport properties and the collision term in the kinetic equation is taken into account to the infinite power in $\underline{K}$ by means of a cumulant expansion. When an approximate solution so obtained is applied to calculation of transport coefficients at a very low density or a high density it is found that the transport coefficients behave[3(a),3(b)] correctly as a function of density when compared with experiment.

The solution obtained by the first-order cumulant approximation for the collision term in the kinetic equation enables us to describe highly nonlinear irreversible processes in terms of the linear transport coefficients appearing in the first-order Chapman-Enskog solution. The theory thus facilitates treatment of nonlinear irreversible processes with no more effort than that which is necessary for linear irreversible processes, at least in the first-order cumulant approximation. It therefore provides a very useful means of reducing and understanding the complexities of nonlinear irreversible processes occurring far from equilibrium situations. In the present study we shall use the nonlinear evolution equations derived from the generalized Boltzmann equation by the modified moment method and solve the resulting generalized hydrodynamic equations for plane Couette flow between plates at different temperatures.[13] As will be seen, there occur some interesting features of nonlinear fluid behavior in a

Lennard-Jones fluid ranging in density from a very dilute to a very high density and at a large Knudsen number; recall the interpretation of mean free path given in a previous paragraph.

The work is organized in the following manner. In Sec. II we present the evolution equations, the equation of state, and the linear transport coefficients for a viscous heat-conducting dense Lennard-Jones gas. These evolution equations can be derived from the generalized Boltzmann equation with the help of the modified moment method. The equation of state and the density and temperature dependences of linear transport coefficients are constructed by gleaning the molecular dynamics data and kinetic-theory results on dense fluids. In Sec. III the evolution equations are cast into a form appropriate for the steady plane Couette flow and the nonlinear shear viscosity and heat-conductivity coefficients are derived from the evolution equations. In Sec. IV we present the results of the numerical solution of the generalized hydrodynamics equations; that is, the velocity and temperature profiles for various flow parameters. The study especially focuses on the characteristic features of nonlinear fluid behavior when the velocity and temperature gradients are high. Section V is for discussion and conclusion.

II. STRESS TENSOR AND HEAT-FLUX EVOLUTION EQUATIONS AND LINEAR TRANSPORT COEFFICIENTS

A. Evolution equations

If the gas is dilute it is sufficient to take into account only isolated binary collisions to describe the evolution of the system toward equilibrium. In that case the Boltzmann equation provides an adequate framework of the kinetic theory of nonequilibrium processes. However, for a dense fluid for which isolated binary collisions are no longer a correct representation of collision events that have got much more complicated owing to a higher density it is necessary to generalize the kinetic equation of Boltzmann to incorporate the higher-order collisions and suitably account for their effects on the evolution of the system toward equilibrium. In the literature there exist some alternatives[14] for the treatment of the dense system. Our analysis is based on the generalized Boltzmann equation proposed by Eu for dense fluids. Various evolution equations can be derived from the generalized Boltzmann equation.[15] The relevant evolution equations for the fluxes necessary for the present problem are[16]

$$\rho\frac{d}{dt}\hat{\underline{P}}=-\vec{\nabla}\cdot\psi^{(1)}+2\rho[\hat{\underline{P}}\cdot\underline{\vec{\gamma}}]^{(2)}+2p\underline{\vec{\gamma}}+2\rho\hat{\Delta}\underline{\vec{\gamma}}-\tfrac{2}{3}\rho\hat{\underline{P}}\vec{\nabla}\cdot\vec{u}+[V^{(2)}]^{(2)}+\Lambda^{(1)}\,, \tag{1}$$

$$\rho\frac{d}{dt}\hat{\Delta}=-\vec{\nabla}\cdot\psi^{(2)}+\tfrac{2}{3}\vec{\vec{P}}:\underline{\vec{\gamma}}-\tfrac{2}{3}\rho\vec{\nabla}\cdot\vec{u}-p\frac{d}{dt}\ln(pv^{5/3})+\tfrac{1}{3}V^{(2)}:\vec{\vec{U}}+\Lambda^{(2)}\,, \tag{2}$$

$$\rho\frac{d}{dt}\hat{\underline{Q}}=-\vec{\nabla}\cdot\psi^{(3)}+\rho^{-1}\vec{\nabla}\cdot\vec{\vec{P}}\cdot(\vec{\vec{P}}-p\vec{\vec{U}})+\vec{Q}\cdot\underline{\vec{\gamma}}+\psi^{(3)}\cdot\underline{\vec{\gamma}}-\vec{\vec{P}}\cdot\vec{\nabla}\hat{h}+V^{(3)}+\Lambda^{(3)}\,, \tag{3}$$

where ρ is the density, $\hat{h}$ is the enthalpy density per unit mass, p is the hydrostatic pressure,

$$\hat{\underline{P}}=[\vec{\vec{P}}]^{(2)}/\rho\,, \tag{4}$$

$$\hat{\Delta}=(\tfrac{1}{3}\mathrm{Tr}\vec{\vec{P}}-p)/\rho\,, \tag{5}$$

$$\hat{\underline{Q}}=\vec{Q}/\rho\,, \tag{6}$$

$$\underline{\vec{\gamma}}=-\tfrac{1}{2}[\vec{\nabla}\vec{u}+(\vec{\nabla}\vec{u})^{t}]+\tfrac{1}{3}\vec{\vec{U}}\mathrm{Tr}\vec{\nabla}\vec{u}\,, \tag{7}$$

$$[\vec{\vec{A}}]^{(2)}=\tfrac{1}{2}(\vec{\vec{A}}+\vec{\vec{A}}^{t})-\tfrac{1}{3}\vec{\vec{U}}\mathrm{Tr}\vec{\vec{A}}\,, \tag{8}$$

and $\psi^{(a)}$, $a=1,2,3$, and $V^{(a)}$, $a=2,3$, are the averages of certain molecular moments and $\Lambda^{(a)}$, $a=1,2,3$, are the dissipation terms related to the entropy production and thus to the collision integral in the kinetic equations. For the details of the quantities given above and those given below in connection with the kinetic theory the reader is referred to Refs. 2 and 16.

In the first-order cumulant approximation the dissipation terms may be written as

$$\Lambda^{(1)}=-(\rho p/\eta_0)\hat{\underline{P}}\sinh\kappa_1/\kappa_1\,, \tag{9a}$$

$$\Lambda^{(2)}=-(\rho p/\eta_{b0})\hat{\Delta}\sinh\kappa_1/\kappa_1\,, \tag{9b}$$

$$\Lambda^{(3)}=-(\rho p\hat{h}/\lambda_0)\hat{\underline{Q}}\sinh\kappa_1/\kappa_1\,, \tag{9c}$$

where $\eta_0,\eta_{b0},\lambda_0$ are linear shear viscosity, bulk viscosity, and heat conductivity of the dense fluid, respectively. Unlike the dilute-gas transport coefficients they depend on the density. The κ_1 is given by

$$\kappa_1^2=\rho^2\beta g[(2\eta_0)^{-1}\hat{\underline{P}}:\hat{\underline{P}}+(\eta_{b0})^{-1}\hat{\Delta}^2+\lambda_0^{-1}\hat{\underline{Q}}\cdot\hat{\underline{Q}}]\,, \tag{10}$$

$$\beta=1/k_BT\,, \tag{11}$$

$$g=(m_r/2k_BT)^{1/2}/n^2\sigma^2\,, \tag{12}$$

with m_r and σ denoting the reduced mass and the size parameter of the molecule and n the number density. The linear transport coefficients generally depend on the temperature as well and their precise form depends on the interaction potential. We will present particular forms for them shortly. If we define the parameters τ_p,τ_b,τ_q by

$$\tau_p=[2\eta_0(m_rk_BT/2)^{1/2}]^{1/2}/nk_BT\sigma\,, \tag{13a}$$

$$\tau_b=[\eta_{b0}(m_rk_BT/2)^{1/2}]^{1/2}/nk_BT\sigma\,, \tag{13b}$$

$$\tau_q=[\lambda_0(m_rk_BT/2)^{1/2}]^{1/2}/nk_BT\sigma\,, \tag{13c}$$

then κ_1 may be written in the following form:

$$\kappa_1=\left[\left[\frac{\tau_p}{2\eta_0}\right]^2\hat{\underline{P}}:\hat{\underline{P}}+\left[\frac{\tau_p}{\eta_{b0}}\right]^2\hat{\Delta}\cdot\hat{\Delta}+\left[\frac{\tau_q}{\lambda_0}\right]^2\hat{\underline{Q}}\cdot\hat{\underline{Q}}\right]^{1/2}. \tag{14}$$

It is easy to show that κ_1 is dimensionless and its square is related to the Rayleigh-Onsager dissipation function. For

more details of (1)—(14) the reader is referred to Refs. 2 and 16.

Equations (1)—(3) together with the equation of state and the mass, momentum, and energy balance equations

$$\frac{\partial}{\partial t}\rho = -\vec{\nabla}\cdot\rho\vec{u}\ , \tag{15}$$

$$\rho\frac{d}{dt}\vec{u} = -\vec{\nabla}\cdot\vec{\vec{P}}\ , \tag{16}$$

$$\rho\frac{d}{dt}E = -\vec{\nabla}\cdot\vec{Q} - \vec{\vec{P}}:\vec{\nabla}\vec{u}\ , \tag{17}$$

completely determine the nonequilibrium evolution of mass, momentum, and energy in the system, provided appropriate boundary and initial conditions are imposed. At this point it would be appropriate to stress that in the entire course of evolution the entropy production in the system is given for the formula

$$\sigma_{\text{ent}} = k_B g^{-1}\kappa_1 \sinh\kappa_1\ , \tag{18}$$

which remains positive irrespective of the magnitude of $\vec{\vec{P}}$ and $\vec{Q}$.

B. Linear transport coefficients and equation of state

In the equations and formulas presented above there appear linear transport coefficients and the pressure. Since they generally depend on density and temperature, their explicit functional form is required to carry out the intended study of the flow properties of the fluid. To obtain their density and temperature dependence explicitly, we assume a Lennard-Jones fluid obeying the Lennard-Jones interaction potential

$$V(r) = 4\epsilon\left[\left[\frac{\sigma}{r}\right]^{12} - \left[\frac{\sigma}{r}\right]^{6}\right]\ ,$$

where ϵ is the well depth and σ is the size parameter. The equation of state of the fluid is extensively investigated to a very high density by means of molecular dynamics. It can be represented, to a good agreement with the experimental results, by the following analytical expression proposed by Ree:[8]

$$\begin{aligned} pV/Nk_BT &= 1+3.629x+7.264x^2+10.4925x^3+11.46x^4+2.176x^{10} \\ &\quad -(1/T^*)^{1/2}(5.369x+13.16x^2+18.525x^3-17.076x^4+9.32x^5) \\ &\quad +(1/T^*)(-3.492x+18.698x^2-35.505x^3+31.816x^4-11.195x^5) \equiv 1+B(x,T^*)\ , \end{aligned} \tag{19}$$

where x is a dimensionless quantity defined by

$$x = (N\sigma^3/V)(\epsilon/k_BT)^{1/4}\ , \tag{20a}$$

which is a function of reduced density and reduced temperature T^* which is defined by

$$T^* = k_BT/\epsilon\ . \tag{20b}$$

Although it is possible in principle to calculate in the framework of kinetic theory the temperature and density[5] dependences of linear transport coefficients by solving many-body dynamics of molecules, in the present investigation we make use of the results obtained by Ashurst and Hoover[6] and Holian *et al.*[7] which may be written in the forms

$$\begin{aligned} \eta_0 &= \{0.171+0.0152[1.0-0.5(1/T^*)^{1/2}+(2/T^*)]\} \\ &\quad \times(\exp\{7.02[1.0-0.2(1/T^*)^{1/2}]x\}-1.0) \\ &\quad \times(m\epsilon)^{1/2}\sigma^{-2}(k_BT/\epsilon)^{2/3}\ , \end{aligned} \tag{21}$$

$$\begin{aligned} \lambda_0 &= \{0.642+0.36[\exp(3.76x)-1.0]\}\sigma^{-2} \\ &\quad \times(\epsilon/m)^{1/2}(k_BT/\epsilon)^{2/3}k_BT\ . \end{aligned} \tag{22}$$

The equation of state and the formulas for linear transport coefficients given above are tested against the available molecular dynamics and experimental data and are found quite satisfactory. The exponential form for the shear viscosity also gets theoretical support from a kinetic-theory investigation[5] on dense-fluid transport coefficients.

Before turning our attention to the nonlinear transport coefficient, let us determine the effective mean free path of a Lennard-Jones fluid. If n_0 is the average density at the average temperature T_0, then we define the effective mean free path l of the Lennard-Jones fluid by the relation

$$\eta_0 = \tfrac{1}{2}\rho\bar{c}l = \tfrac{1}{2}mn_0\bar{c}l\ , \tag{23}$$

where $\bar{c}$ is the mean value of the peculiar velocity and can be approximated by the following expression:

$$\bar{c} = \left[\frac{8k_BT_0}{\pi m}\right]^{1/2}\ . \tag{24}$$

Substituting (21) and (24) in (23) we get

$$\begin{aligned} l &= \left[0.2147+0.019\,08\left[1-\frac{0.5}{(T_0^*)^{1/2}}+\frac{2.0}{T_0^*}\right]\right. \\ &\quad \left.\times\left\{\exp\left[7.02\left[1-\frac{0.2}{(T_0^*)^{1/2}}\right]x_0\right]-1\right\}\right]\frac{(T_0^*)^{1/6}}{n_0\sigma^2}\ , \end{aligned} \tag{25a}$$

where

$$x_0=\frac{n_0\sigma^3}{(T_0^*)^{1/4}} . \tag{25b}$$

We can rewrite (25) as

$$l=\frac{0.2147}{n_0\sigma^2}[1+F_1(x_0,T_0^*)] , \tag{26}$$

where

$$F_1(x_0,T_0^*)=0.0888\left[1-\frac{0.5}{(T_0^*)^{1/2}}+\frac{2.0}{T_0^*}\right] \times\left\{\exp\left[7.02\left[1-\frac{0.2}{(T_0^*)^{1/2}}\right]x_0\right]-1\right\} . \tag{27}$$

We shall see in our subsequent analysis that the flow properties of the Lennard-Jones fluid intricately depend on the "effective Knudsen number," defined as

$$\underline{K}=\frac{l}{L}=\frac{0.2147}{n_0\sigma^2}(T_0^*)^{1/6}\frac{[1+F_1(x_0,T_0^*)]}{L} , \tag{28}$$

where L is the macroscopic length scale characterizing the geometry of the flow system. We would in particular investigate two limiting cases when $\underline{K}$ is large. These are the following.

(a) The case when the pressure is very low ($\lesssim 1$ Pa at room temperature). In this case of a very dilute gas the Knudsen number

$$\underline{K}\approx\frac{0.2147}{n_0\sigma^2}\frac{(T_0^*)^{1/6}}{L} \tag{29}$$

is very large due to very low gas density. An understanding of the flow characteristics at this limit would be of interest.

(b) At the other extreme we would examine the flow dynamics of a very dense gas, when the gas is subjected to a very high temperature difference and a large viscous stress over a very small distance, say, of an order of a micron. The flow characteristic in this extreme would provide some insight into the nature of the nonlinear effects which one might observe in the shock-wave profile in a dense gas.

III. NONLINEAR TRANSPORT COEFFICIENTS AND THE GENERALIZED HYDRODYNAMIC EQUATIONS FOR PLANE COUETTE FLOW

A. Generalized hydrodynamic equations

To put the nonlinear evolution equations in more manageable forms we now take a specific flow problem. Consider a steady plane Couette flow of a fluid between infinite parallel plates maintained at two different temperatures. The upper plate is moving at a constant velocity and its direction will be taken as the direction of the x axis in the Cartesian coordinate system. The lower plate is fixed at a distance D away from the moving plate; see

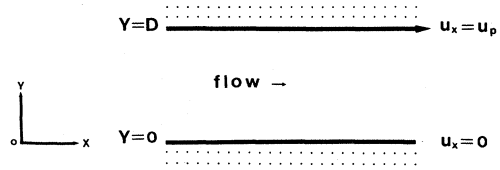

FIG. 1. Flow geometry. The upper plate is moving along the x axis at speed u_p.

Fig. 1. Therefore there is a temperature gradient in the transversal direction of the flow. It is assumed that the temperature is uniform in the x direction. There is no transversal component of the velocity, but the x component has a gradient in the y direction. Consequently, the velocity and the temperature are functions of y only, the pressure can be shown to remain constant as will be shown below, the mass balance equation is identically satisfied, and the bulk viscosity has no role to play since the divergence of velocity is identically equal to zero. This allows us to drop the evolution equation of the excess trace of the stress tensor $\overleftrightarrow{P}$ from consideration. We therefore have two evolution equations (1) and (3) to consider for the fluxes.

Let us define the nonlinear shear viscosity η and the nonlinear heat conductivity coefficient λ by the following relations:

$$\mathring{\underline{P}}\equiv\rho\hat{\underline{P}}=2\eta\overleftrightarrow{\underline{\gamma}} , \tag{30}$$

$$\vec{Q}=-\lambda\vec{\nabla}\ln T . \tag{31}$$

Since the stress tensor and the heat flux are generally nonlinear functions of the rate-of-strain tensor and the temperature gradient if the processes are nonlinear, the nonlinear transport coefficients η and λ just defined are functions of the shear rate

$$\gamma=(\overleftrightarrow{\underline{\gamma}}:\overleftrightarrow{\underline{\gamma}})^{1/2}/\sqrt{2} \tag{32}$$

and the absolute value of the temperature gradient

$$\chi=|\vec{\nabla}\ln T| . \tag{33}$$

Only in the limit of γ and χ small compared to the characteristic time and length, respectively, will the relations in (30) and (31) reduce to the familiar relations holding for Newtonian flow and Fourier heat conduction.

Equations (1)—(3) are three lower-order moment equations since the stress tensor and the heat flux are a second and a third moment, respectively, in the language of the moment method. In this method the entire set of moments is assumed to give completely the distribution function in question. However, since the set is infinite, it is in practice suitably truncated either on a physical ground or by a mathematical approximation. From the experimental standpoint most macroscopic processes observed for simple fluids appear possible to describe in terms of the first thirteen moments which include the density, velocity, internal energy, stress tensor, and heat flux. Therefore, if we assume that the thirteen moments are sufficient for the

description of the macroscopic behavior of a simple fluid and if we also assume that the distribution function is a functional of the thirteen moments evolving according to the moment evolution equations, then it is appropriate to drop the higher-order moments appearing in the evolution equations instead of expressing them in terms of the thirteen moments chosen. The latter approach is taken in the conventional moment method and in the modified moment method up until now, but we propose to simply neglect them since it appears logically more consistent to do so than to keep and express them in terms of the lower-order moments. In this connection it must be recalled that the distribution function is given in terms of the thirteen moments and the dissipative terms $\Lambda^{(a)}$ are calculated in terms of the thirteen moments alone. Then, since $\psi^{(a)}$, $\psi^{(3)}$, and $V^{(a)}$ are in fact higher-order moments that are not included in the distribution function, we simply put them equal to zero in the thirteen moment approximation,

$$\psi^{(a)}=0, \quad a=1,2,3$$
$$V^{(a)}=0, \quad a=1,2 . \tag{34}$$
$$\psi^{(3)}=0 .$$

Since at the steady state and for the geometry of flow under consideration

$$\frac{d\vec{u}}{dt}=0 ,$$

we see that

$$\vec{\nabla}\cdot\vec{\mathbf{P}}\cdot(\vec{\mathbf{P}}-p\vec{\mathbf{U}})=0 . \tag{35}$$

Moreover, by (30) and for the reason of the flow geometry

$$(\vec{\mathbf{P}}\cdot\vec{\nabla}\hat{\mathbf{h}})_y=p\nabla_y\hat{\mathbf{h}}+2\eta(\vec{\underline{\gamma}}\cdot\vec{\nabla}\hat{\mathbf{h}})_y$$
$$=p\nabla_y\hat{\mathbf{h}} . \tag{36}$$

When these facts are taken into consideration, the steady-state evolution equations for the plane Couette flow are reduced to the forms

$$0=p-(p\eta/\eta_0)\sinh\kappa_1/\kappa_1 , \tag{37}$$
$$0=p\hat{\mathbf{h}}-(p\hat{\mathbf{h}}\lambda/\lambda_0)\sinh\kappa_1/\kappa_1 , \tag{38}$$

where κ_1 now may be expressed

$$\kappa_1=[2(\tau_p\gamma)^2(\eta/\eta_0)^2+(\tau_q\chi)^2(\lambda/\lambda_0)^2]^{1/2} . \tag{39}$$

For the plane Couette flow

$$\gamma=\tfrac{1}{2}\,|\,\partial u_x/\partial y\,| , \tag{40}$$
$$\chi=|\,\partial\ln T/\partial y\,| . \tag{41}$$

We rewrite (37) and (38) as

$$\eta(\sinh\kappa_1/\kappa_1)=\eta_0 , \tag{42}$$
$$\lambda(\sinh\kappa_1/\kappa_1)=\lambda_0 . \tag{43}$$

To solve these equations, we take the square of each equation and add the resulting equations after multiplying each of them with the factor $(\sqrt{2}\tau_p/\eta_0)^2$ and $(\tau_q/\lambda_0)^2$, respectively. We then obtain

$$\sinh^2[(\sqrt{2}\tau_p\gamma\eta/\eta_0)^2+(\tau_q\chi\lambda/\lambda_0)^2]$$
$$=(\sqrt{2}\tau_p\gamma)^2+(\tau_q\chi)^2 . \tag{44}$$

A particular solution of this equation is

$$\eta=\eta_0\sinh^{-1}\frac{[(\sqrt{2}\tau_p\gamma)^2+(\tau_q\chi)^2]^{1/2}}{[(\sqrt{2}\tau_p\gamma)^2+(\tau_q\chi)^2]^{1/2}} . \tag{45}$$

$$\lambda=\lambda_0\sinh^{-1}\frac{[(\sqrt{2}\tau_p\gamma)^2+(\tau_q\chi)^2]^{1/2}}{[(\sqrt{2}\tau_p\gamma)^2+(\tau_q\chi)^2]^{1/2}} . \tag{46}$$

By using (40) and (41), we may make the gradient dependence more explicit in the equations above,

$$\eta=\eta_0\sinh^{-1}\kappa/\kappa , \tag{47}$$
$$\lambda=\lambda_0\sinh^{-1}\kappa/\kappa , \tag{48}$$
$$\kappa=\{[\tfrac{1}{2}\tau_p(\partial u_x/\partial y)]^2+[\tau_q(\partial\ln T/\partial y)]^2\}^{1/2} . \tag{49}$$

By introducing a simplifying notation

$$q_e=\sinh^{-1}\kappa/\kappa \tag{50}$$

we shall often write the nonlinear transport coefficients in more compact forms,

$$\eta=\eta_0 q_e , \tag{51}$$
$$\lambda=\lambda_0 q_e . \tag{52}$$

Here we would like to add that q_e is a measure of the nonlinearity of the nonequilibrium dissipative processes. In the case of the linear dissipative processes $q_e=1$ and the farther the system is removed from the linear domain, the smaller the value of q_e will be. Apart from the thermodynamic gradients, q_e depends on the temperature and density of the fluid. To analyze this aspect properly, we now focus our attention on the expressions of τ_p and τ_q. Especially the density dependence is contained in the factors τ_p and τ_q which are proportional to $\sqrt{\eta_0}/n$ and $\sqrt{\lambda_0}/n$, respectively. Since the transport coefficients generally increase sharply—exponentially, in fact—as the density increases, the factors will increase with the density on account of the transport coefficients, and they will also increase as the density approaches zero on account of the factor $(1/n)$ since in the limit the linear transport coefficients tend to density-independent values. To see the density and temperature dependence of q_e more clearly, it is useful to rearrange (19) into the form

$$1/nk_BT=(\sigma^3/\epsilon p^*)[1+B(x,T^*)] , \tag{53}$$

where

$$p^*=p\sigma^3/\epsilon , \tag{54}$$

a reduced pressure. Substituting (53) and (21) into (13a) we get

$$\tau_p=(m/\epsilon\sqrt{2})^{1/2}\sigma(0.342+0.0304(1-0.5/\sqrt{T^*}+2.0/T^*)\times\{\exp[7.02(1-0.2/\sqrt{T^*})x]-1\})^{1/2}(1+B)(T^*)^{7/12}/p^* . \quad (55)$$

Similarly, by using (53) and (22) in (13b) we get

$$\tau_q=\sigma(1/2)^{1/4}\{1.284+0.72[\exp(3.76x)-1]\}^{1/2}\times(1+B)(T^*)^{13/12}/p^* . \quad (56)$$

With the help of (55), (56), (49), and (50) we can now express q_e in the following manner:

$$q_e=\sinh^{-1}\kappa/\kappa , \quad (57)$$

$$\kappa=2.2904\underline{K}\,\underline{M}(\gamma_0 T_2^*)^{1/2}(T_0^*)^{-7/6}\left[\frac{1+B(x,T^*)}{1+B(x_0,T_0^*)}\right]\times\left[\frac{[1+F_1(x,T^*)]}{2[1+F_1(x_0,T_0^*)]}(T^*)^{7/6}\left[\frac{du^*}{d\xi}\right]^2+\frac{1.877(T^*)^{1/6}}{\underline{M}^2\gamma_0 T_2^*}\cdot\frac{[1+F_2(x,T^*)]}{[1+F_1(x_0,T_0^*)]}\left[\frac{dT^*}{d\xi}\right]^2\right]^{1/2} , \quad (58)$$

$$F_1(x,T^*)=0.088\,89(1-0.5/\sqrt{T^*}+2/T^*)\times\{\exp[7.02(1-0.2/\sqrt{T^*})x]-1\} , \quad (59)$$

$$F_2(x,T^*)=0.5607[\exp(3.76x)-1] , \quad (60)$$

$$\underline{M}=u_p/(\gamma_0 R T_2)^{1/2} , \quad (61)$$

$$\gamma_0=C_p/C_v . \quad (62)$$

It is clear from (57) and (58) that the nonlinearity index q_e is greatly influenced by the dimensionless parameters $\underline{M},\underline{K}$ and the imposed temperature difference $T_2^*-T_1^*$. As any one of these parameters increases, the function q_e deviates from unity and hence the nonlinear transport coefficients accordingly deviate from the linear transport coefficient. In such cases, to understand the flow dynamics, one has to solve the generalized hydrodynamic equation.

Having discussed the various quantities appearing in q_e, we now consider the balance equations. In the case of the plane Couette flow described in Fig. 1, the mass, momentum, and energy balance equations may be written as

$$\frac{\partial}{\partial y}\rho u_x=0 , \quad (63)$$

$$\frac{\partial}{\partial y}\eta\frac{\partial u_x}{\partial y}=0 , \quad (64a)$$

$$\frac{\partial}{\partial y}\left[\lambda\frac{\partial}{\partial y}\ln T\right]+\eta\left[\frac{\partial u_x}{\partial y}\right]^2=0 . \quad (64b)$$

For the problem under consideration

$$\frac{\partial p}{\partial y}=0 . \quad (65)$$

Since $u_x=u_x(y)$ for the plane Couette flow here, we obtain from (63)

$$u_x\frac{\partial\rho}{\partial x}=0 ,$$

which implies

$$\frac{\partial\rho}{\partial x}=0 \text{ or } \frac{\partial n}{\partial x}=0 \quad (66)$$

since $u_x=0$ in general. Equation (66) means that n is a function of y. Since by virtue of the problem in hand

$$\frac{\partial T}{\partial x}=0 , \quad (67)$$

the equation of state, (66), and (67) imply that

$$\frac{\partial p}{\partial x}=0 . \quad (68)$$

Therefore, the pressure remains constant and the density profile may be computed in terms of the temperature profile. In view of this result we find it sufficient to solve (64a) and (64b) for $u_x(y)$ and $T(y)$.

B. Boundary conditions

The generalized hydrodynamic equations (64a) and (64b) are subject to boundary conditions which are derived as described below. To arrive at the boundary conditions, we examine collisions between the wall surface and the gas molecules which occur regardless of the gas density.

It is well known through numerous investigations[17–19] on interfacial phenomena that the surface exerts a long-range attractive force on the gas molecules and as a consequence the gas molecules get adsorbed and then desorbed. There may be possible even chemisorption through which the chemical nature of the gas may be changed. In any event, these processes drive the gas molecules to reach thermal and mechanical equilibrium with the wall. It is therefore possible to see that the boundary values of gas temperature and velocity can be determined if the interfacial interactions are taken into consideration. This idea was implemented in a previous paper[19(c)] in which the boundary temperature and velocity values are calculated along the line similar to the theory of Langmuir. Since the details of the theory are available in the paper[19(c)] quoted above, we shall omit the derivation and simply present only the final results along with some explanatory remarks.

Through interfacial interactions a fraction θ of molecules reach thermal equilibrium with the wall at the surface. Then the fraction of the gas molecules leaving the surface without reaching thermal equilibrium with the wall but at the same temperature as the incident molecules is $(1-\theta)$. This fraction θ can be shown to have the form

$$\theta = bp/(1+bp) , \tag{69}$$

where p is the gas pressure and the parameter b depends on the wall temperature and the interfacial interaction parameters. It is obtained as follows. We regard the surface-gas molecule interaction process as a chemical reaction leading to a quasistable complex of a surface particle and a molecule,

$$S + M \rightleftarrows SM ,$$

where S, M, and SM, respectively, denote the surface particle (site), the gas molecules, and the complex formed between the surface particle and the gas molecule. Then it can be shown that b is related to the chemical equilibrium constant K for the chemical reaction and consequently the partition functions of S, M, and SM,

$$\begin{aligned} b &= K/k_B T_W \\ &= (V q_{SM}/q_S q_M)/k_B T_W , \end{aligned} \tag{70}$$

where T_W is the wall temperature and q_i is the partition function of i. In a model which treats the complex as a particle moving, subjected to a constant potential of depth D_e, in a box of size Al where A is the mean area of a site (S) and l is the mean free path, the partition functions may be easily calculated and we find

$$b = (Al/k_B T_W)\exp(D_e/k_B T_W) . \tag{71}$$

When the gas pressure is so low that the mean free path is as long as the gap D between the two plates, we may take l with $D/2$. The reason for this choice was given elsewhere,[20(c)] but it suffices to say that it is a mean collision distance between the wall surface and the gas molecules impinging at all angles. In that case we obtain

$$b = (AD/2k_B T_W)\exp(D_e/k_B T_W) . \tag{72}$$

The potential parameter D_e and the mean area A can be inferred from various experimental data on interfacial phenomena.

With θ so determined, we calculate the boundary values for temperature and velocity which in the case of the present flow geometry are as follows: at $y=0$,

$$\begin{aligned} T &= \theta(T_1)T_1 + [1-\theta(T_1)]T_g , \\ u &= [1-\theta(T_1)]u_p/2 , \end{aligned} \tag{73a}$$

at $y=D$,

$$\begin{aligned} T &= \theta(T_2)T_2 + [1-\theta(T_2)]T_g , \\ u &= [1+\theta(T_2)]u_p/2 , \end{aligned} \tag{73b}$$

where we may take

$$T_g = (T_1+T_2)/2 .$$

The fraction θ depends on the gas pressure; as p increases, θ tends to unity. In fact the value of b is such that θ is practically equal to unity at the normal pressure, but as the pressure decreases, the value of θ increasingly deviates from unity as shown in Fig. 2(a). We therefore see that

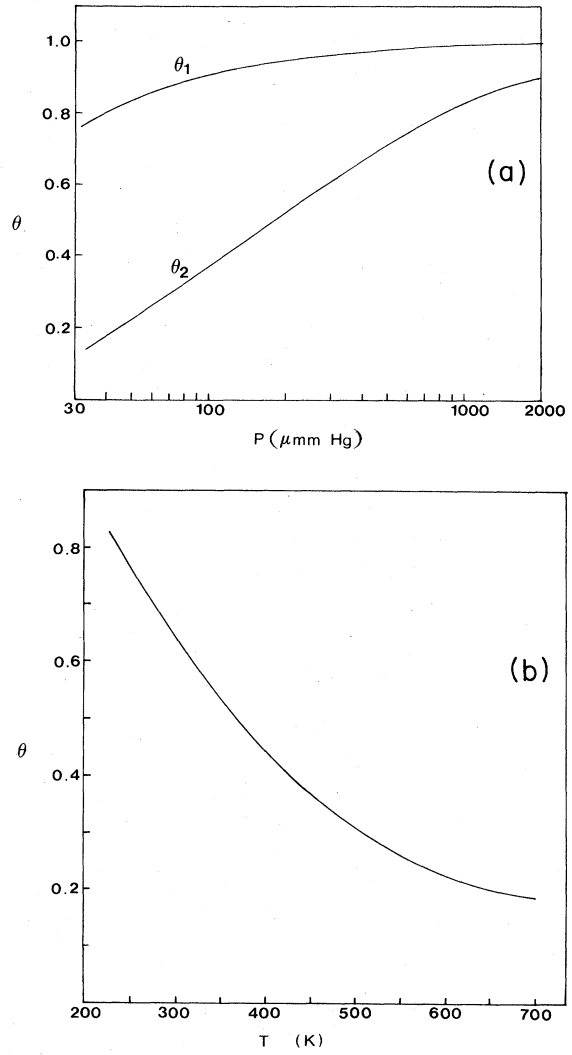

FIG. 2. (a) Fraction θ of thermalized molecules in the interface is plotted as a function of pressure. θ_1 is for the lower plate ($T_1=288$ K) and θ_2 is for the upper plate ($T_2=4T_1$). No slip-boundary conditions correspond to $\theta=1$. (b) Fraction θ of thermalized molecules in the interface is plotted as a function of temperature. $p=20\,\mu$mm Hg.

the boundary conditions (73a) and (73b) tend to exhibit slips as the pressure decreases, whereas they become those of stick boundary conditions as the pressure increases toward the normal value and beyond. In gas dynamics the slip boundary conditions (i.e., the case of $\theta \neq 1$) are taken if the gas is rarefied, whereas the stick boundary conditions (i.e., the case of $\theta=1$) are taken if the gas density is normal. This manner of taking of boundary conditions leaves the transition regime of density in limbo and makes the gas dynamics for such a regime rather awkward to handle. The present theory of boundary conditions removes such a difficulty and facilitates fluid dynamic treatment of the entire density range with a uniform formalism. In Fig. 2(b) is presented the temperature depen-

dence of θ which decreases with an increasing T. This behavior implies that the temperature and velocity slip increase as the wall temperature increases. This may be understood if it is realized that as the temperature increases, the residence time of the complex gets shorter and thus the chance for its reaching equilibrium with the wall is reduced.

IV. SOLUTION OF THE GENERALIZED HYDRODYNAMIC EQUATIONS

Equations (64a) and (64b) may be cast into a little more convenient form. For this purpose we observe that since for arbitrary u_x

$$u_x \frac{\partial}{\partial y}\eta\frac{\partial u_x}{\partial y}=0 , \tag{74}$$

adding it to (64b), we get

$$\frac{\partial}{\partial y}\left[\lambda\frac{\partial}{\partial y}\ln T\right]+\eta\left[\frac{\partial u_x}{\partial y}\right]^2+u_x\frac{\partial}{\partial y}\eta\frac{\partial u_x}{\partial y}=0 ,$$

which may be written as

$$\frac{\partial}{\partial y}\left[\left[\lambda\frac{\partial}{\partial y}\ln T\right]_x\eta\frac{\partial u_x}{\partial y}\right]=0 .$$

The hydrodynamic equations to be solved are then as follows:

$$\frac{\partial}{\partial y}\left[\eta\frac{\partial u_x}{\partial y}\right]=0 , \tag{75a}$$

$$\frac{\partial}{\partial y}\left[\lambda\frac{\partial \ln T}{\partial y}+u_x\eta\frac{\partial u_x}{\partial y}\right]=0 . \tag{75b}$$

Integrating the above equations once, we obtain

$$\eta\frac{\partial u_x}{\partial y}=C_1 , \tag{76}$$

$$\lambda\frac{\partial \ln T}{\partial y}+u_x\eta\frac{\partial u_x}{\partial y}=C_2 , \tag{77}$$

where C_1 and C_2 are constant. By using (76) in the second term of (77), we simplify it further,

$$\lambda\frac{\partial \ln T}{\partial y}=C_2-C_1u_x . \tag{78}$$

By using the dimensionless variables introduced before and substituting forms for nonlinear viscosity and heat conductivity, we finally express the steady-state generalized hydrodynamic equations for a dense nonlinear Lennard-Jones fluid in the following forms:

$$q_e(0.171+0.0152(1-0.5/\sqrt{T^*}+2/T^*)\times\{\exp[7.02(1-0.2/\sqrt{T^*})x]-1\})(T^*)^{2/3}\frac{du^*}{d\xi}=C_1 , \tag{79}$$

$$q_e\{0.642+0.36[\exp(3.76x)-1]\}(T^*)^{2/3}\frac{dT^*}{d\xi}=C_2-C_1\underline{E}u^* , \tag{80}$$

where

$$\underline{E}=\gamma_0 T_2^*\underline{M}^2$$

and q_e is given by (57). Equations (76) and (78) are solved by a numerical method for various values of the parameter set $(\underline{K},\underline{M},T_1^*,T_2^*,p^*)$. The boundary conditions for (76) and (77) or (78) are already discussed. At each step of solution we determine the density by solving the equation of state which in a nondimensional form can be written as

$$\begin{aligned}p^*=&(T^*)^{5/4}x(1+3.629x+7.264x^2+10.4925x^3+11.46x^4+2.176x^{10})\\&-(T^*)^{3/4}(5.369x^2+13.16x^3+18.525x^4-17.076x^5+9.32x^6)\\&+(T^*)^{3/4}(-3.492x^2+18.698x^3-35.505x^4+31.816x^5-11.195x^6) .\end{aligned} \tag{81}$$

Note that x depends on T^* as well as $N^*=N\sigma^3/V$ and hence $x(T^*)^{5/4}=n^*T^*$.

Equations (79) and (80) cover the case of the fluid at low densities down to the rarefied regime, provided the inertia terms can be neglected. (That may not be allowed for some cases of flow.) As the density vanishes, the linear shear viscosity η_0 and the linear heat conductivity λ_0 become independent of density whereas

$$q_e^*\sim n^*\ln[(n^*)^{-1}] \tag{82}$$

apart from a factor independent of n^*. More precisely, in the very low density regime

$$q_e=\sinh^{-1}\kappa_0/\kappa_0\equiv q_e^* , \tag{83}$$

$$\begin{aligned}\kappa_0=&\nu^*[\tfrac{1}{2}(T^*)^{7/6}(du^*/d\xi)^2\\&+1.8771(T^*)^{1/6}\underline{E}^{-1}(dT^*/d\xi)^2]^{1/2} ,\\ \nu^*=&2.2904\underline{K}\,\underline{M}(\gamma_0T_2^*)^{1/2}(T_0^*)^{-7/6} .\end{aligned} \tag{84}$$

The generalized hydrodynamic equations then take the simpler forms as follows:

$$0.171q_e^*(T^*)^{2/3}\frac{du^*}{d\xi}=C_1 , \tag{85}$$

$$0.642q_e^*(T^*)^{2/3}\frac{dT^*}{d\xi}=C_2-C_1\underline{E}u^* . \tag{86}$$

These equations have also been numerically solved. The solutions provide the velocity and temperature profiles for

the plane Couette flow of a dilute Lennard-Jones gas.

Let us divide (86) side by side with (85) to obtain

$$a\frac{dT^*}{du^*}=\frac{C_2}{C_1}-\underline{E}u^*,\quad a=0.642/0.171\ . \tag{87}$$

This equation may be integrated easily,

$$aT^*=\frac{C_2}{C_1}u^*-\tfrac{1}{2}\underline{E}(u^*)^2+C_3\ . \tag{88}$$

Since at $\xi=0$, $T^*=T_1^*$ and $u^*=0$, we obtain

$$aT_1^*=C_3\ . \tag{89}$$

At $\xi=1$, $T^*=T_2^*$ and $u^*=1$. Therefore

$$aT_2^*=\frac{C_2}{C_1}-\tfrac{1}{2}\underline{E}+aT_1^* \tag{90}$$

or

$$\frac{C_2}{C_1}=a\,\Delta T+\tfrac{1}{2}\underline{E}\ . \tag{91}$$

We finally obtain the following relation between T^* and u^*:

$$a(T^*-T_1^*)=(a\,\Delta T+\tfrac{1}{2}\underline{E})(u^*)-\tfrac{1}{2}\underline{E}(u^*)^2\ , \tag{92}$$

which suggests that T is a parabolic function of u^* with a maximum at

$$u^*=(a\,\Delta T+\tfrac{1}{2}\underline{E}) \tag{93}$$

and its value given by

$$T^*_{\max}=T_1^*+(a\,\Delta T+\tfrac{1}{2}\underline{E})^2/2\underline{E}a\ . \tag{94}$$

This relation holds for both linear and nonlinear processes.

It was shown in a previous paper[4] that the fluid-dynamical approach to flow profiles for rarefied Maxwell gases yields correct results in the low-Knudsen- and Mach-number region where comparison was possible with the kinetic-theory results by Liu and Lees.[20] They obtained their results for Maxwell gases by solving approximately the linearized Boltzmann equation in terms of two stream local-equilibrium distribution functions and moment equations for conserved variables. Therefore, encouraged by the comparison already made, we will further carry on calculation of flow profiles to understand the effects of thermoviscous coupling and nonlinear transport coefficients on flow profiles of a Lennard-Jones gas. The numerical solutions are obtained by a combination of the Runge-Kutta-Gill method and the shooting method in which the slopes of temperature and velocity at a boundary are so adjusted that the boundary conditions at the other boundary are satisfied.

A. Dilute gas

When the slip boundary conditions are used, the values of $\theta(T_1)\equiv\theta_1$ and $\theta(T_2)\equiv\theta_2$ appearing in (73a) and (73b) are evaluated, except for the case of Fig. 3, with the following parameter values for D_e and A:

$$D_e=1.32\ \text{kcal/mol}\ ,$$

$$A=5\times10^{-15}\ \text{cm}^2\ ,$$

$$D=0.13\ \text{cm}\ .$$

These values are inferred from the experimental data available in the literature on the Al-Ar system.[17–19] The boundary conditions for the present theory are calculated with the parameters given above.

In a previous paper[4] we calculated various profiles for a Maxwell gas by using the same method. Here, to see the effect of a different potential model we have calculated the flow profiles for the parameter set $\underline{M}=3$, $\underline{K}=0.238$, $T_1^*=2.2$, $T_2^*=8.8$. The results of this calculation are presented in Fig. 3.

The solid curves correspond to the solution of the generalized hydrodynamic equations with the boundary conditions obtained by Liu and Lees[20] in their kinetic theory of a rarefied Maxwell gas. The result obtained with the linear theory for which $q_e=1$ is represented by the broken lines. It is seen that flow profiles for nonlinear transport processes are different from those of the linear theory. According to the comparison made in the paper[4] on a Maxwell gas the flow profiles obtained by Liu and Lees (represented by circles) are essentially the flow profiles one obtains in the linear theory. Consequently, a slight deviation between linear temperature profiles and those of Liu and Lees can be attributed to the difference in the potential models since Liu and Lees use the Maxwell model for the interaction potential whereas in the present studies a Lennard-Jones potential has been used. We base this on

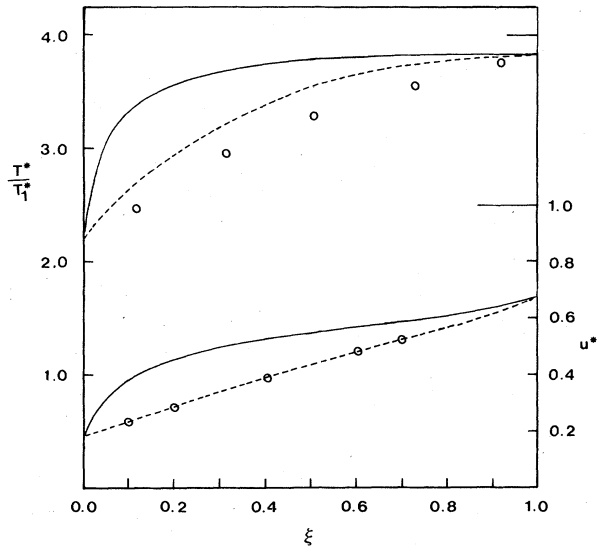

FIG. 3. Velocity and temperature profiles computed with the boundary conditions coinciding with those by Liu and Lees (Ref. 17): $u_1^*=0.17$, $T^*=5.10$, $u_2=0.66$, $T_2^*=8.83$. Other parameters are $\underline{K}=0.238$, $\underline{M}=3$, $T_1=2.32$, $T_2=4T_1$. The solid curves are the nonlinear theory profiles while the broken curves are the linear theory profiles. The circles are the values given by the Liu-Lees theory for the Maxwell gas.

the fact that the present theory gives excellent agreement with the Liu-Lees results in the case of a Maxwell model as shown previously.[4] We also observe that near the lower plate there is a steep change in temperature and velocity which may be regarded as a boundary layer in which most of the nonlinear irreversible processes occur. To verify this we increase the nonlinearity and investigate the flow profiles in the case of $\underline{M}=6.0$. Note that an increase in the Mach number increases the nonlinearity. The flow profiles for these cases are presented in Fig. 4. The existence of boundary layers at both walls are more evident now. In fact, except for thin layers from the walls the temperature and the velocity are almost constant in a fashion characteristic of rarefied gas flows, viz., in the mainstream the fluid behaves as an inviscid fluid since the velocity gradient is approximately equal to zero. The existence of the boundary layers stems from the gradient-sensitive nonlinear transport coefficients and it is interesting to note that the boundary layer becomes thinner as the Mach number increases. The behavior is in agreement with the recent analysis[21] of a relation between the boundary layer structure and the nonlinear transport processes as considered in this paper. According to the analysis, the reduced boundary layer (nondimensional, similarity solution) becomes thinner as $\underline{K}\,\underline{M}$ increases. This is in contrast to the boundary-layer thickness calculated with the Navier-Stokes equations which predict[22] the reduced boundary layer profile independent of $\underline{K}$ and $\underline{M}$. The linear flow profiles do not have thin boundary-layer structures for the parameter values chosen. The reason that the nonlinear temperature profiles tend to be flatter than the linear profiles can be understood by the fact that the nonlinear thermal conductivity is generally smaller than

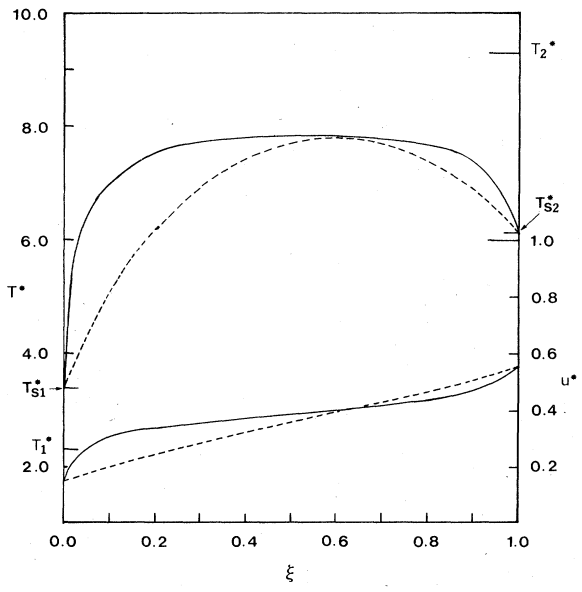

FIG. 4. Velocity and temperature profiles calculated with the boundary conditions (73a) and (73b): $u_1^*=0.15$, $T_{S1}^*=3.38$, $u_2^*=0.547$, $T_{S2}^*=6.13$. The potential parameters are $D_e=1.32$ kcal/mol and $A=5\times10^{-15}$ cm^2. Other parameters are $\underline{K}=0.238$, $\underline{M}=6$, $T_1^*=2.32$, $T_2^*=9.28$.

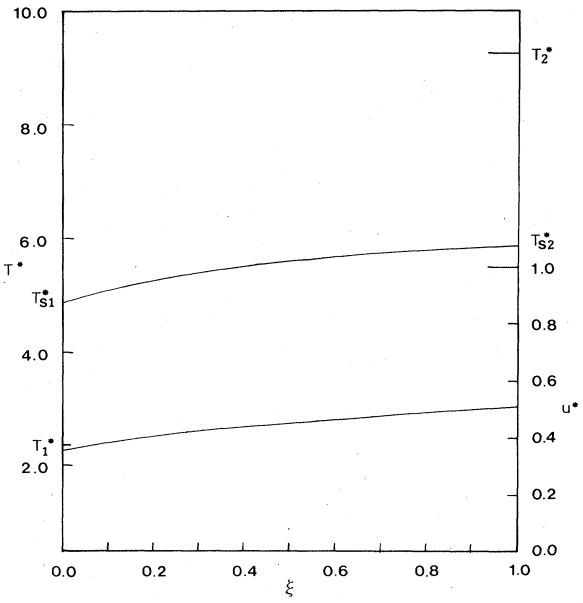

FIG. 5. Velocity and temperature profiles for $\underline{K}=1.51$, $\underline{M}=3$, $T_1^*=2.32$, $T_2^*=9.28$, $p=3.41$ μmm Hg. The boundary conditions in this case turn out to be $u_1^*=0.36$, $T_{S1}^*=4.88$; $u_2^*=0.51$, $T_{S2}^*=5.85$.

the linear heat conductivity. Because of this fact, the heat due to the viscous heating effect is accumulated in the midstream. This has an interesting implication since it can be inferred that less heat is transferred to the boundary from the midstream in the case of the nonlinear heat conduction.

In Fig. 5 we investigate the flow profiles of a highly rarefied gas with a large Knudsen number. The tempera-

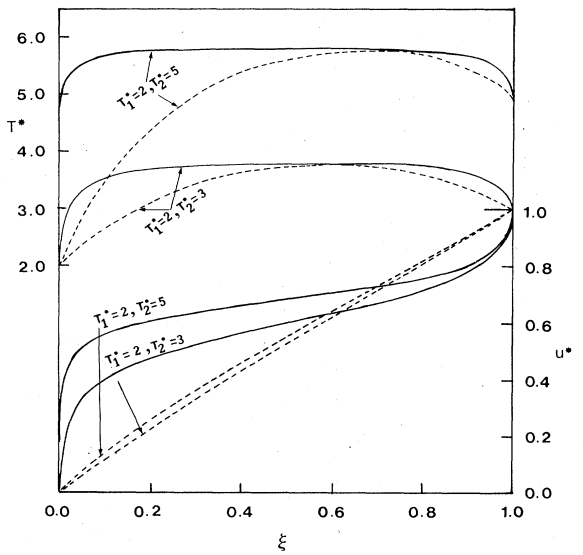

FIG. 6. Velocity and temperature profiles for different plate temperatures in the case of $\underline{K}=1.05$, $\underline{M}=2.68$. The profiles are calculated with no slip-boundary conditions.

ture and velocity slips are calculated with (73a) and (73b). In this particular case the temperature and velocity gradients are considerably reduced owing to a large slip at the walls. As a result the nonlinear profiles are indistinguishable from the linear flow profiles. Once again, the velocity and temperature profiles are practically constant almost everywhere.

The velocity profile at a normal density calculated from the Navier-Stokes equation with no slip-boundary condition suggests that in the Couette-flow geometry most of the gas follows the hot plate because the gas viscosity is large there owing to the fact that the viscosity increases with the temperature. According to Liu and Lees,[20] this

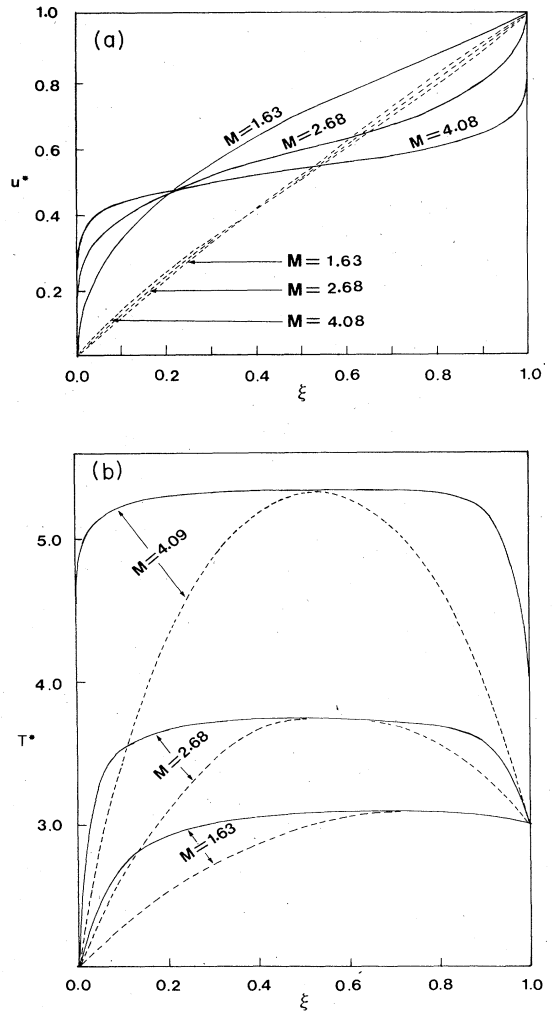

FIG. 7. (a) Velocity profiles for different Mach numbers. The solid curves are the nonlinear theory profiles while the broken curves are the linear theory profiles. The no-slip-boundary conditions are used and $\underline{K}=1.05$, $T_1^*=2$, $T_2^*=3$. (b) Temperature profiles for different Mach numbers. The solid and broken curves are, respectively, the nonlinear and the linear theory profiles. The no-slip-boundary conditions are used and $\underline{K}=1.05$, $T_1^*=2$, $T_2^*=3$.

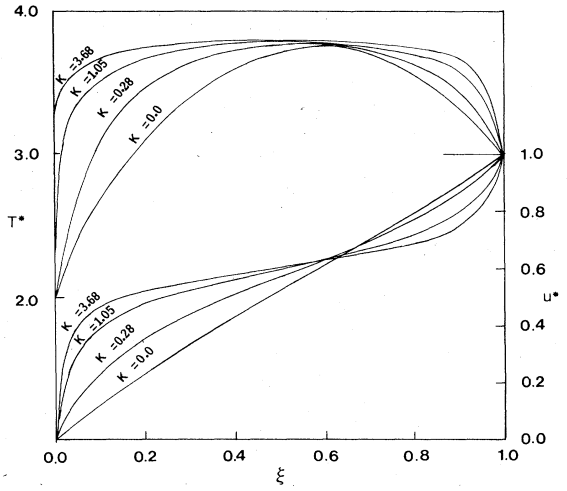

FIG. 8. $\underline{K}$ dependence of velocity and temperature profiles in the case of $\underline{M}=2.68$, $T_1^*=2.0$, and $T_2^*=3.0$. No-slip-boundary conditions are used.

situation is reversed in highly rarefied gases where most of the gas would follow the cold plate because the velocity slip is larger at the hotter plate than at the colder plate.

However, the results in Fig. 5 indicate that the prediction of Liu and Lees may not be true in general. Part of the problem may lie in the fact that Liu and Lees might be overestimating the velocity slip at the upper wall. It also appears that their theory of slip gives well-behaved results only when the Mach number and the Knudsen number are relatively small.

We now focus our attention on the flow characteristic of high-speed rarefied-gas flows when the nature of the surface is such that the velocity and temperature slips are negligible. That is, $\theta(T_1)=\theta(T_2)=1$.

In Fig. 6 we investigate the effect of the temperature

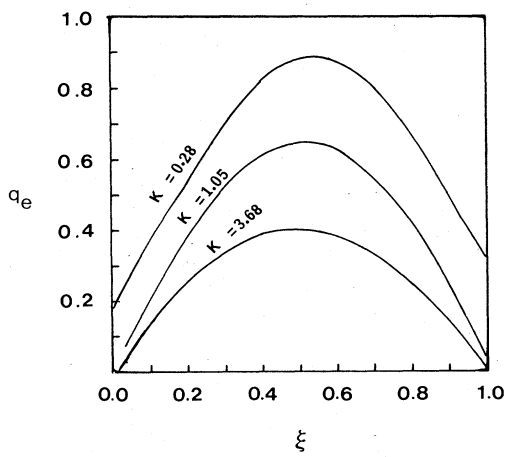

FIG. 9. Nonlinearity factor q_e vs ξ for different values of $\underline{K}$ in the case of $\underline{M}=2.68$, $T_1^*=2$, and $T_2^*=3$.

difference $\Delta T = T_2^* - T_1^*$. Since ΔT is also a measure of nonlinearity we see that the temperature and velocity profiles tend to exhibit the characteristics typical of nonlinear transport processes observed in other situations studied so far; cf. Figs. 3–5. Observe that the velocity profiles get significantly affected by an increased ΔT, and this is one of the thermoviscous-coupling effects. The solid curves are nonlinear theory profiles while the broken curves are linear profiles.

The flow profiles with no slip conditions are presented in Figs. 7–9. In Figs. 7(a) and 7(b), where the solid curves are nonlinear theory profiles and the broken curves are linear theory profiles, we investigate the effects of variation in the Mach number. It is seen that as the velocity of the upper plate increases, the velocity and thermal boundary layers become more and more pronounced. Similarly, as shown in Fig. 8, as the Knudsen number is increased the rarefaction increases and the nonlinear features become more pronounced. In Fig. 9 the variation of the nonlinear index q_e is shown from which it can be deduced that the nonlinear transport coefficients go through a remarkably large variation over the interval [0,1]. Both η and λ get small in magnitude as $\underline{K}$ increases. In the hope of checking the correctness of the numerical method used and also gaining some further insight into the velocity profiles we have plotted in Fig. 10 the temperature-velocity correlation curves. They correspond to traces of the values of T^* and u^* in the interval $0 \leq \xi \leq 1$ for the two different sets of (T_1^*, T_2^*) presented in Fig. 4. As predicted by the analytical result (92), both linear and nonlinear profiles for T^* and u^* trace a single correlation curve. The only difference between the linear and nonlinear profile is different locations on the curve for the (T^*, u^*) sets at the same value of ξ. The numerals accompanying the symbols on the curve indicate an ascending sequence of the ξ value. The linear (T^*, u^*) (0) set lags behind the nonlinear (T^*, u^*) (x) set until the maximum is reached but the relative positions are reversed after the maximum is passed. This analysis of numerical solutions strengthens the confidence in the numerical accuracy of the results.

Based on the flow profiles obtained from the generalized hydrodynamic equations with no slip conditions, we may infer that the velocity and the temperature jump near the wall in the rarefied-gas regime which are identified as the velocity and the temperature slip, may be a direct consequence of the nonlinear transport coefficients. Thus to understand the slip phenomena we have not only to undertake a detailed examination of the gas-surface interactions, but also to recognize the influence of nonlinear transport coefficients in high-speed rarefied-gas flow regime. We remark that the kind of nonlinear transport processes considered here has not been taken into consideration in slip-flow phenomena in the past.

B. Dense gas

We now turn to investigate the flow characteristics of a very dense Lennard-Jones fluid. Such an analysis, in spite of its special geometry, would give some idea about the nonlinear effects arising, for example, in shock-wave propagation in a dense fluid. In these experiments the enormous change in pressure and temperature occur over a microscale and consequently the linear transport theory is no longer adequate for the macroscopic description of dissipative processes in such flow systems.

To calculate the flow profiles of a dense gas, we solve

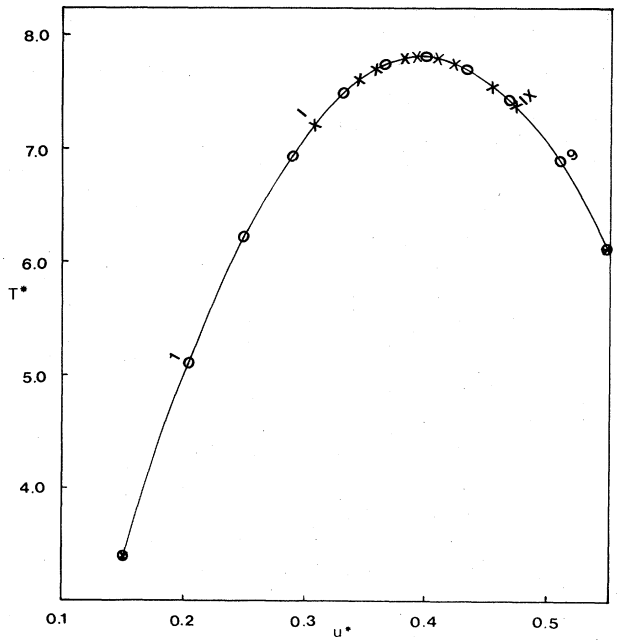

FIG. 10. Temperature-velocity phase diagram obtained from the profiles in Fig. 4.

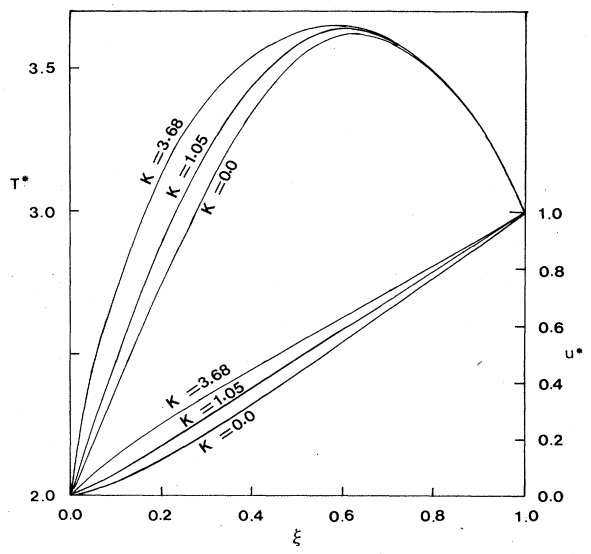

FIG. 11. Velocity and temperature profiles for a dense Lennard-Jones gas. The parameters are $p^* = 5$, $T_1^* = 2$, $T_2^* = 3$, $\underline{M} = 2.68$.

the generalized hydrodynamic equations (76) and (78) in which the transport coefficients are given by the density-dependent nonlinear viscosity and thermal-conductivity formulas already presented. The boundary conditions are formally the same as for the dilute gas, but they are practically the no-slip boundary conditions since the fractions $\theta(T_1)$ and $\theta(T_2)$ are virtually equal to unity; cf. Fig. 2. The pressure is described by the equation of state (81) for the Lennard-Jones fluid.

In Fig. 11 the effect of the increase in the effective Knudsen number on the flow properties of a dense fluid is studied, with the rest of the parameters given by $\underline{M}=2.68$, $T_1^*=2.0$, $T_2^*=3.0$, $p^*=5.0$. The values of $\underline{K}$ taken are 1.05 and 3.68. We remark that $\underline{K}$ in these cases is the effective Knudsen number as defined in (28). As is evident from the figure, the velocity and temperature profiles for nonlinear transport processes deviate considerably from the corresponding flow profiles calculated with the help of the linear theory for which $q_e=1$. However, in contrast to the rarefied-gas flows described, there is no evidence for the existence of boundary layers in this particular case. It is also observed that the excessive viscous heating due to the viscous dissipation of the kinetic energy decreases the gas density near the upper plate and thereby nonlinear effects are reduced. In Fig. 12 we investigate the influence of pressure on the flow profiles. Once again there are considerable differences between the flow profiles for nonlinear and linear transport processes. As the pressure increases, the fluid becomes less mobile and therefore the velocity profiles are becoming convex downward whereas the temperature profiles are raised due to an increased energy dissipation into heat. In Fig. 13 the variations of density-dependent linear and nonlinear transport coefficients with respect to ξ are presented. The parameter set used is $p^*=5$, $T_1^*=2.0$, $T_2^*=3.0$, $\underline{M}=2.68$, $\underline{K}=3.68$. The nonlinear shear viscosity and heat conductivity are considerably smaller than the corresponding linear values. These transport coefficients are local and strongly depend on ξ. It may also be noticed that unlike the case of rarefied-gas flows where the fluid behaves as inviscid in the mainstream, the dense fluid exhibits appreciable dissipative effects in the mainstream, exhibiting no flat portions in the profiles. We again stress that $\underline{K}$ in the case of Figs. 11–13 for the dense fluids stands for the effective Knudsen number defined with the effective mean free path over which the momentum or the energy is carried in the fluid. This length is not so short in the case of a dense fluid owing to a relatively long correlation length on account of intimate interactions of particles.

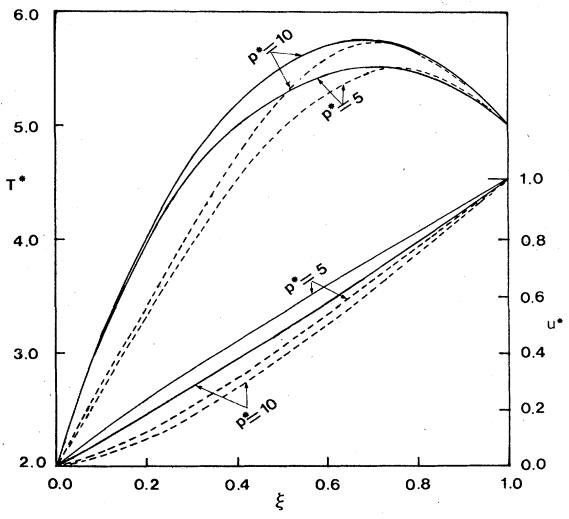

FIG. 12. Velocity and temperature profiles for a dense Lennard-Jones gas at different pressures. The other parameters are $\underline{K}=1.05$, $\underline{M}=2.68$, $T_1^*=2$, and $T_2^*=5$.

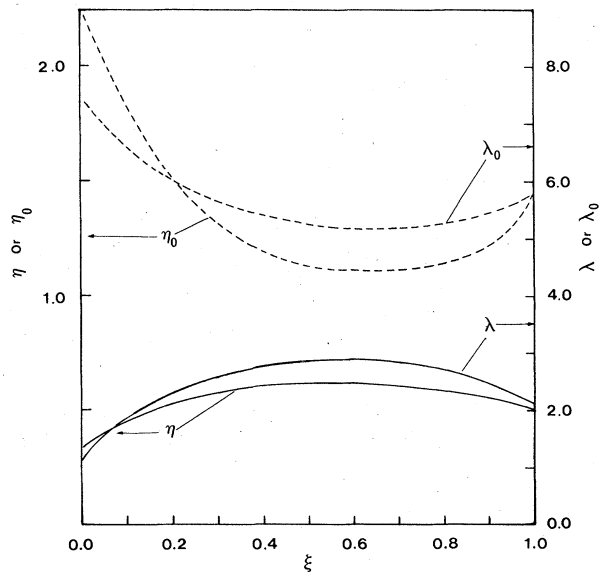

FIG. 13. ξ dependence of linear and nonlinear transport coefficients for a dense Lennard-Jones gas. The parameters are $p^*=5$, $T_1^*=2$, $T_2^*=3$, $\underline{M}=2.68$, $\underline{K}=3.68$, and $\nu^*=17.4$. The linear and nonlinear transport coefficients have qualitatively different ξ dependences which have significantly different effects on the profiles.

V. DISCUSSION AND CONCLUSION

The aim of the present work is in studying the effect of the nonlinear transport coefficients on the velocity and temperature profiles for a Lennard-Jones fluid. There are, however, a number of significant aspects of fluid dynamics in connection with the present work that must be discussed.

A. Nonlinear-transport coefficients and slip phenomena

The nonlinear transport coefficients obtained in this work and in the modified moment method in general are dependent on thermodynamic gradients. Therefore they are not constant in contrast to the linear transport coefficients to which they reduce as the thermodynamic gra-

dients decrease in magnitude. The thermodynamic-gradient dependence of nonlinear transport coefficients gets noticeable as τ_p and τ_q get large. The latter can be large since they are inversely proportional to the density if the density is small, or since the linear transport coefficients become very large owing to the increase in the molecular correlation length if the density is high. [Note that the transport coefficients increase exponentially with the density; see (21) and (22).] Either way, the velocity and temperature profiles show pronounced deviations from the predictions by the theory that is based on the linear transport coefficients of dilute gases. Historically, the linear transport coefficients[23] have been calculated by means of the mean-free-path-theory of Clausius, Maxwell's kinetic theory, or the first-order Chapman-Enskog solution[10] of the Boltzmann kinetic equation. All of these theories predict density-independent transport coefficients which in turn, with the help of hydrodynamic equations, predict constant gradients. Yet as the density is reduced to a sufficiently low value (e.g., 50 μmm Hg in pressure) and as the Knudsen number gets large, one finds evidence of the linear laws breaking down and the "slipping" of the velocity and the temperature at the wall. Maxwell's theory[24(a)] of slip phenomena was an attempt to make a correction to the constant linear transport coefficients, and later theories[24(b)–24(d)] by others are, in essence, in the same kind of spirit, and are within the framework of the theory of linear transport processes, regardless of whether boundary conditions are imposed on the distribution function or not. (Maxwell's theory does not impose boundary conditions on the distribution function whereas more recent theories by later authors do.)

The theory of nonlinear transport processes on which the present calculations are based provides an alternative method of handling the flow phenomena[25] for all densities. This theory is different from the existing theories[24] in that it acknowledges the importance of the gas-surface interaction and the basically nonlinear nature of the slip problem by solving the kinetic equation accordingly to reflect the nonlinear nature. The use of a cumulant expansion for the entropy production is ultimately a declaration of such a recognition, and its correctness appears to be indicated by the velocity and temperature profiles which manifestly exhibit a boundary-layer structure at the wall.

B. Comparison of the nonlinear transport coefficients with those in Maxwell's theory

To understand the nature of the nonlinear transport coefficients (47) and (48) used in the present theory, we compare them with the effective transport coefficients deduced from the Maxwell theory[24] of slip phenomena. To facilitate a closer comparison, we shall assume that there is no coupling between viscosity and heat conductivity and consider only the viscosity. Thus in the case of no temperature gradient the nonlinear viscosity coefficient is given by

$$\eta=\eta_0\sinh^{-1}(\tau\gamma)/\tau\gamma \ ,$$
$$\tau=\tau_p/2 \ ,$$
$$\gamma=\partial u_x/\partial y=U\,\partial u^*/\partial\xi\equiv U\gamma^* \ .$$

If the reduced quantities defined in (55)—(63) are used, the argument of the inverse hyperbolic function may be written as

$$\tau\gamma=\nu_2\underline{K}(\partial u^*/\partial\xi)\equiv\nu_2\underline{K}\gamma^* \ ,$$

where

$$\nu_2=1.61\gamma_0^{1/2}(T^*)^{-1/12}\underline{M} \ .$$

Note that the Knudsen number is inversely proportional to the density.

The nonlinear viscosity in terms of the reduced quantities is

$$\eta=\eta_0\sinh^{-1}(\nu_2\underline{K}\gamma^*)/\nu_2\underline{K}\gamma^*$$
$$=\eta_0\ln\{\nu_2\underline{K}\gamma^*+[1+(\nu_2\underline{K}\gamma^*)^2]^{1/2}\}/\nu_2\underline{K}\gamma^* \ . \quad (95)$$

On the other hand, in the Maxwell theory of slip flow the velocity near the wall is given to first order of $\underline{K}$ by

$$\vec{u}=\vec{u}_0(1-a\underline{K}\gamma^*) \ , \quad (96)$$

where $\vec{u}_0$ is the velocity at the wall and a is a parameter independent of γ^*. This velocity profile implies the viscosity in the form

$$\eta=\eta_0/(1+2a\underline{K}) \ . \quad (97)$$

This is an effective viscosity formula that we wish to compare with (95). There is an important difference between them since η in (95) depends on γ^* whereas η in (97) does not, at least in the order of approximation made for (96). However, both formulas (95) and (97) predict a viscosity vanishing as n increases. In this sense they are similar in their density dependence. As the density decreases, $\underline{K}$ increases and thus η vanishes in both cases, with (95)

$$\eta\sim n\ln n^{-1} \quad (98)$$

and with (97)

$$\eta\sim n \ , \quad (99)$$

both of which mean that the rarefied gas becomes practically inviscid, as is well known. Therefore in such a range of density the fluid behavior is practically that of an inviscid fluid except for thin layers near the walls confining the gas. In the thin boundary layers the viscosity, however small it may be, must be taken into account when the profiles are calculated.

A similar comparison holds for thermal conductivity.

C. Conclusion

The present work fills the lacunae left by the previous work on a Maxwell gas. Here we have studied the velocity and temperature profiles for both dense and dilute thermoviscous Lennard-Jones gases. Density and temperature-dependent linear viscosity and thermal conductivity coefficients are used as well as a virial equation of state proposed by Ree on the empirical ground. The calculations presented show that there are significant nonlinear effects on velocity and temperature profiles that arise when the nonlinear nature of transport processes is

taken into account in hydrodynamics. The theory employed provides, in effect, an alternative method of studying flow problems since the present method is a unified hydrodynamic theory for flow problems ranging in the density from the rarefied to the dense-gas regime. This unification is made possible by the theory of boundary values that enables us to calculate the boundary conditions in terms of the surface-gas molecule interaction parameters. This approach has not been taken before in fluid dynamics. Although we have considered the simplest kind of flow geometry in the present work, the implications of this work would probably hold generally for other types of flow geometry. This line of work is still interesting and worth studying further.

ACKNOWLEDGMENT

The financial support by the Natural Sciences and Engineering Research Council of Canada is gratefully acknowledged.

---

*Also at Physics Department, McGill University, 3600 University Street, Montreal, Quebec H3A 2T8.

[1]See, for example, S. R. de Groot and P. Mazur, *Nonequilibrium Thermodynamics* (North-Holland, Amsterdam, 1962).

[2]B. C. Eu, J. Chem. Phys. **73**, 2958 (1980); **74**, 2998 (1981); **74**, 3006 (1981); **80**, 2123 (1984); **82**, 4283 (1985).

[3](a) B. C. Eu, J. Chem. Phys. **79**, 2315 (1983); (b) B. C. Eu and Y. G. Ohr, J. Chem. Phys. **81**, 2756 (1984); (c) B. C. Eu and A. S. Wagh, Phys. Rev. B **27**, 1037 (1983); (d) B. C. Eu, Phys. Fluids **28**, 222 (1985).

[4]B. C. Eu, R. Khayat, G. D. Billing, and C. Nyeland (unpublished).

[5]B. C. Eu, Ann. Phys. (N.Y.) **120**, 423 (1979).

[6]W. T. Ashurst and W. G. Hoover, Phys. Rev. A **11**, 658 (1975).

[7]B. L. Holian, W. G. Hoover, B. Moran, and G. K. Straub, Phys. Rev. A **22**, 2798 (1980).

[8]F. H. Ree, J. Chem. Phys. **73**, 5401 (1980).

[9]D. Levesque and L. Verlet, Phys. Rev. **182**, 307 (1969); J.-P. Hansen and L. Verlet, Phys. Rev. Lett **184**, 151 (1969).

[10](a) S. Chapman and T. G. Cowling, *Mathematical Theory of Nonuniform Gases,* 3rd ed. (Cambridge, London, 1972); (b) J. H. Ferziger and H. G. Kaper, *Mathematical Theory of Transport Processes in Gases* (North-Holland, Amsterdam, 1972),

[11]H. Grad, Commun. Pure Appl. Math. **2**, 331 (1949).

[12]M. N. Kogan, *Rarefied Gas Dynamics* (Plenum, New York, 1969).

[13]For previous studies on a similar flow problem that, however, use Navier-Stokes equations instead of the generalized hydrodynamic equations, and a model temperature dependence for transport coefficients, see (a) H. C. Levy, Quart. Appl. Math. **7**, 25 (1954); (b) T. Y.-T. Wu, *ibid.* **13**, 393 (1958); (c) A. Sakurai, Quart, J. Mech. Appl. Math. **11**, 274 (1958); (d) N. C. Freeman and S. Kumar, J. Fluid Mech. **56**, 523 (1972).

[14](a) K. Kawasaki and I. Oppenheim, Phys. Rev. **136**, A1519 (1964); **139**, A649 (1965); (b) M. H. Ernst, B. Cichocki, J. R. Dorfman, J. Sharma, and H. van Beijeren, J. Stat. Phys. **18**, 237 (1978), (c) G. Jagannathan, J. S. Dahler, and W. Sung, J. Chem. Phys. **83**, 1808 (1985).

[15]B. C. Eu, Ann. Phys. (N.Y.) **118**, 187 (1979).

[16]B. C. Eu, J. Chem. Phys. **74**, 6362 (1981).

[17](a) I. Langmuir, Phys. Rev. **8**, 149 (1916); (b) S. Dushman, *Scientific Foundation of Vacuum Technique* (Wiley, New York, 1962).

[18](a) F. O. Goodman and H. Y. Wachman, *Dynamics of Gas Surface Scattering* (Academic, New York, 1976); (b) G. A. Somorjai, *Chemistry in Two Dimensions: Surfaces* (Cornell University, Ithaca, 1981).

[19](a) *Fundamentals of Gas Surface Interactions* edited by Saltsburg, J. N. Smith, and M. Rogers (Academic, New York, 1967); (b) W. P. Teagan and G. S. Springer, Phys. Fluids **11**, 4971 (1968); (c) B. C. Eu, D. K. Bhattacharya and R. Khayat (unpublished).

[20]C. Y. Liu and L. Lees, *Rarefied Gas Dynamics,* edited by L. Talbot (Academic, New York, 1961), p. 341.

[21]B. C. Eu (unpublished).

[22]H. Schlichting, *Boundary-Layer Theory,* 7th ed. (McGraw-Hill, New York, 1979).

[23]See S. Chapman and T. G. Cowling [Ref. 10(a)] and J. H. Ferziger and H. G. Kaper [Ref. 10(b)] for some historical accounts; see also E. H. Kennard, *Kinetic Theory of Gases* (McGraw-Hill, New York, 1938).

[24](a) J. C. Maxwell, *Collected Works of J. C. Maxwell* (Cambridge University, London, 1927), Vol. II, p. 86; (b) M. V. Smoluchowski, Wiedemann's Ann. Phys. (Leipzig) **64**, 101 (1898); (c) P. Welander, Arkiv, Fys. **7**, 507 (1954); (d) E. P. Gross, E. A. Jackson, and S. Ziering, Ann. Phys. (N.Y.) **1**, 141 (1957).

[25]For old but interesting experimental articles on slip phenomena, see (a) F. Soddy and A. S. Berry, Proc. R. Soc. London **83**, 254 (1909); (b) W. Mandell and J. West, Proc. Phys. Soc. London **37**, 20 (1925).